SUPPLEMENTAL MATERIAL

Steering the Magnetic Properties of Ni@NiO@CoO Core-Shell Nanoparticle Films: the Role of Core-shell Interface *vs*. Interparticle Interactions

Alessandro Ponti, Anna M. Ferretti, Elena Capetti, Maria Chiara Spadaro, Giovanni Bertoni, Vincenzo Grillo, Paola Luches, Sergio Valeri, Sergio D'Addato

*Theoretical basis of the Δ*M *method*

Consider a collection of single-domain magnetic nanoparticles having some form of magnetic anisotropy. The temperature is low enough that these nanoparticles display magnetic hysteresis. In general, an infinitesimal change dH of the magnetic field applied to such a collection causes a variation of the magnetization dM, which we subdivide into two contributions arising from reversible and irreversible processes

$$\mathrm{d}M = (\mathrm{d}M)_{\mathrm{irr}} + (\mathrm{d}M)_{\mathrm{rev}} \, . \tag{1}$$

In a major hysteresis loop separately consider the descending branch M_{d} (from $+M_{\mathrm{s}}$ to $-M_{\mathrm{s}}$) and the ascending branch M_{a} (from $-M_{\mathrm{s}}$ to $+M_{\mathrm{s}}$). For each branch, we can write

$$\mathrm{d}M_{\mathrm{d}} = (\mathrm{d}M_{\mathrm{d}})_{\mathrm{irr}} + (\mathrm{d}M_{\mathrm{d}})_{\mathrm{rev}} \quad \text{and} \quad \mathrm{d}M_{\mathrm{a}} = (\mathrm{d}M_{\mathrm{a}})_{\mathrm{irr}} + (\mathrm{d}M_{\mathrm{a}})_{\mathrm{rev}}. \tag{2}$$

Suppose now that the increments dM_{d} and dM_{a} are measured at the same applied field H, *i. e.*, they correspond to the infinitesimal intervals of the hysteresis loop between H and H + dH. If we assume that $(\mathrm{d}M_{\mathrm{d}})_{\mathrm{rev}} = (\mathrm{d}M_{\mathrm{a}})_{\mathrm{rev}}$, then

$$\mathrm{d}\Delta M = \mathrm{d}M_{\mathrm{d}} - \mathrm{d}M_{\mathrm{a}} = (\mathrm{d}M_{\mathrm{d}})_{\mathrm{irr}} - (\mathrm{d}M_{\mathrm{a}})_{\mathrm{irr}}. \tag{3}$$

where $\Delta M = M_{\mathrm{d}} - M_{\mathrm{a}}$, as usual. This is a good approximation for non-interacting Stoner-Wohlfarth nanoparticles as shown in the Supporting Information. Dividing by the field increment dH, we obtain the derivatives

$$\frac{d\Delta M}{dH} = \left(\frac{dM_d}{dH}\right)_{irr} - \left(\frac{dM_a}{dH}\right)_{irr} \tag{4}$$

Thus, $d\Delta M/dH$ approximately represents the irreversible changes of the magnetization per unit field. Moreover, there usually is no irreversible magnetization change in the $H \geq 0$ part of M_d and in the $H \leq 0$ part of M_a, so we can write

$$\frac{d\Delta M}{dH} = \begin{cases} -\left(\frac{dM_a}{dH}\right)_{irr} & H \geq 0 \\ \left(\frac{dM_d}{dH}\right)_{irr} & H \leq 0 \end{cases} \tag{5}$$

This is rigorously valid for Stoner-Wohlfarth particles but it reasonably applies to more general cases.

Under these assumptions, the absolute value of $d\Delta M/dH$ corresponds to the distribution of the nanoparticle switching fields obtained by differentiating the DCD curve. It approximately represents the true switching field distribution since interparticle interactions are not taken into account.

Comparison of TRM with and without a magnet reset.

The negative TRM measured at high temperature is an artifact due to the hysteresis of the magnet superconducting coils, as already reported in [1]. A magnet reset carried out at 5 K after switching off the saturating field prevents the occurrence of such artifacts. Unfortunately, the magnet reset cannot be performed during the unattended magnetometer operation usually employed for long experiments such as the thermal behavior of the TRM. We could however show that the position and width of the peak of the TRM derivative $-dM_{TRM}/dT$ are hardly affected by the artifacts.

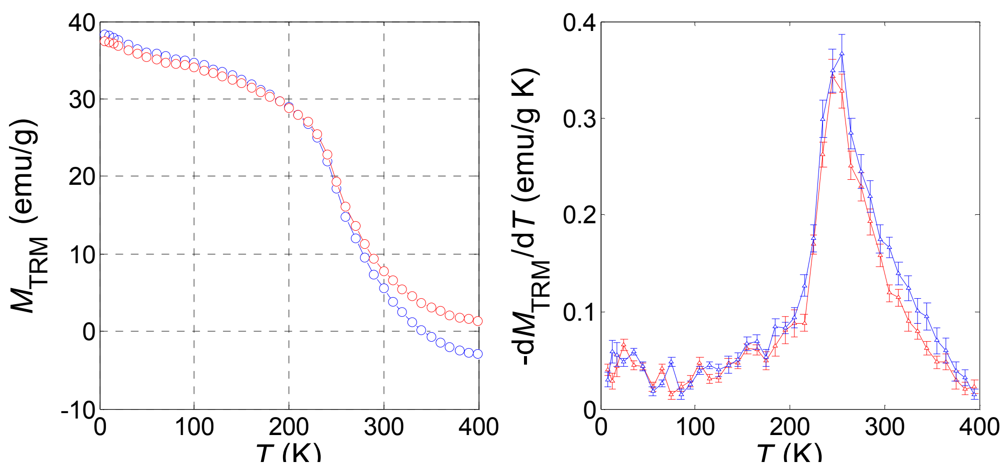

Fig. S1. Comparison of M_{TRM} (left) and $-dM_{TRM}/dT$ (right) of sample B_2 with (red) and without (blue) a magnet reset performed after switching off the saturating field at low temperature. H_{cool} = 100 Oe.

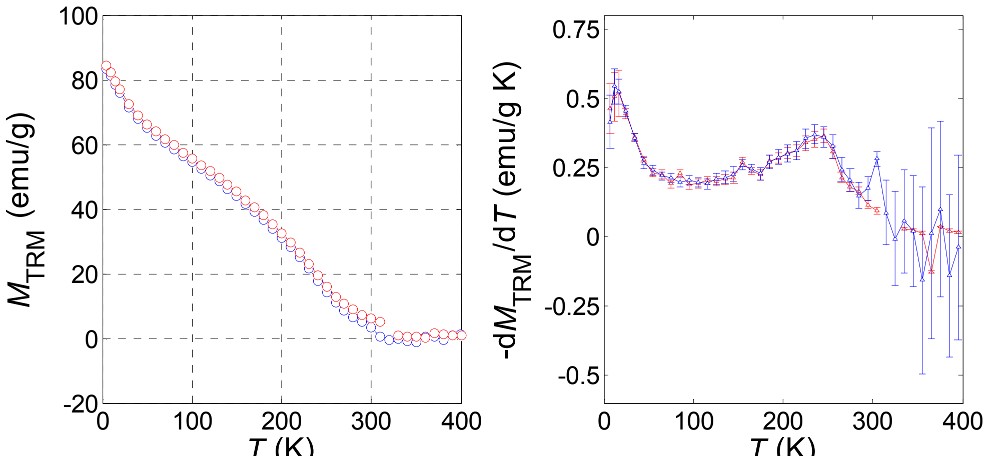

Figure S2. Comparison of M_{TRM} (top) and $-dM_{TRM}/dT$ (bottom) of sample B_2 with (left) and without (right) a magnet reset performed after switching off the saturating field at low temperature. H_{cool} = 10 kOe.

Table SI. Comparison of T_{der} of sample B_2 calculated from TRM data with and without a magnet reset performed after switching off the saturating field at low temperature.

	T_{der} (K)	
	H_{cool} = 100 Oe	H_{cool} = 10 kOe
With magnet reset	240	230
Without magnet reset	250	230

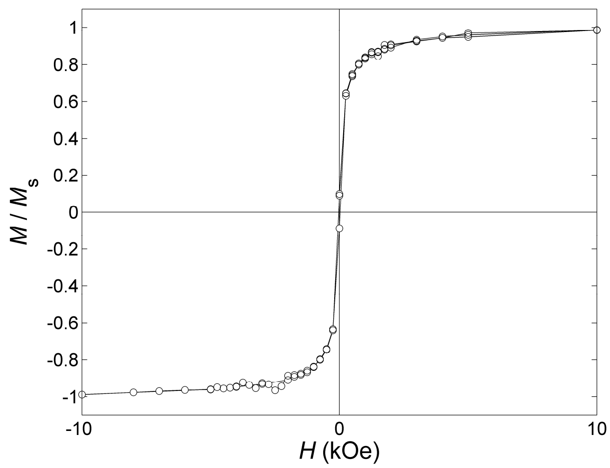

Fig. S3. Magnetization isotherm of sample D recorded at 300 K.

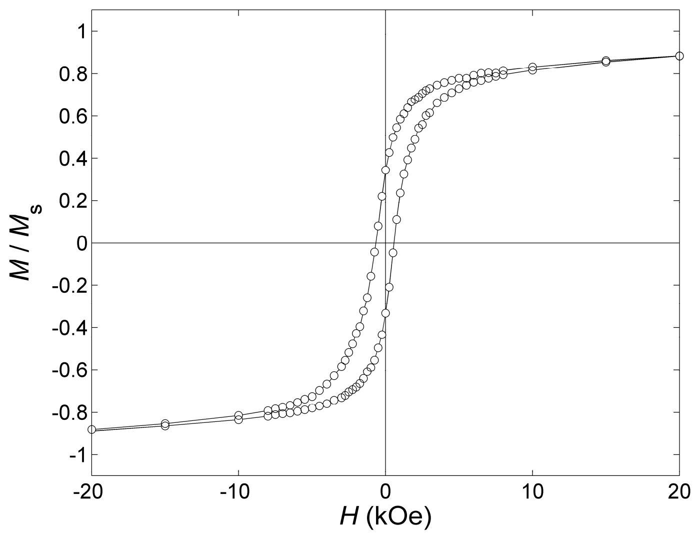

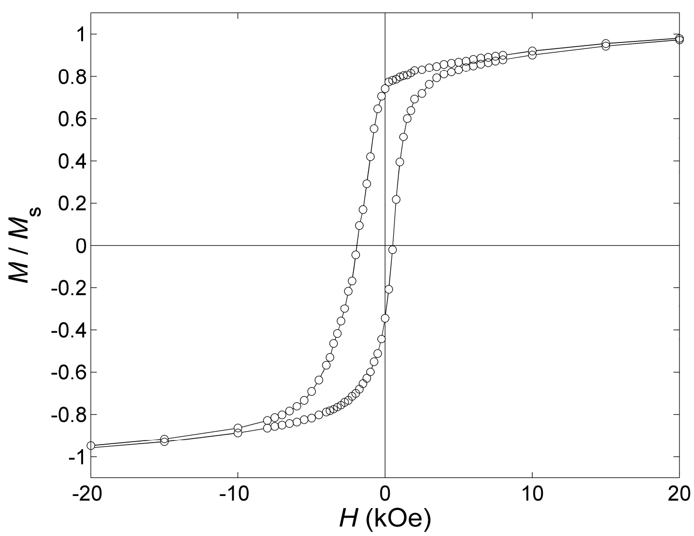

Fig. S4. Comparison of the magnetization isotherms (hysteresis loops) of sample B_2 recorded at 5 K in ZFC (top) and FC (bottom) mode.

Definitions of remanent magnetization M_r for exchange-biased hysteresis loops

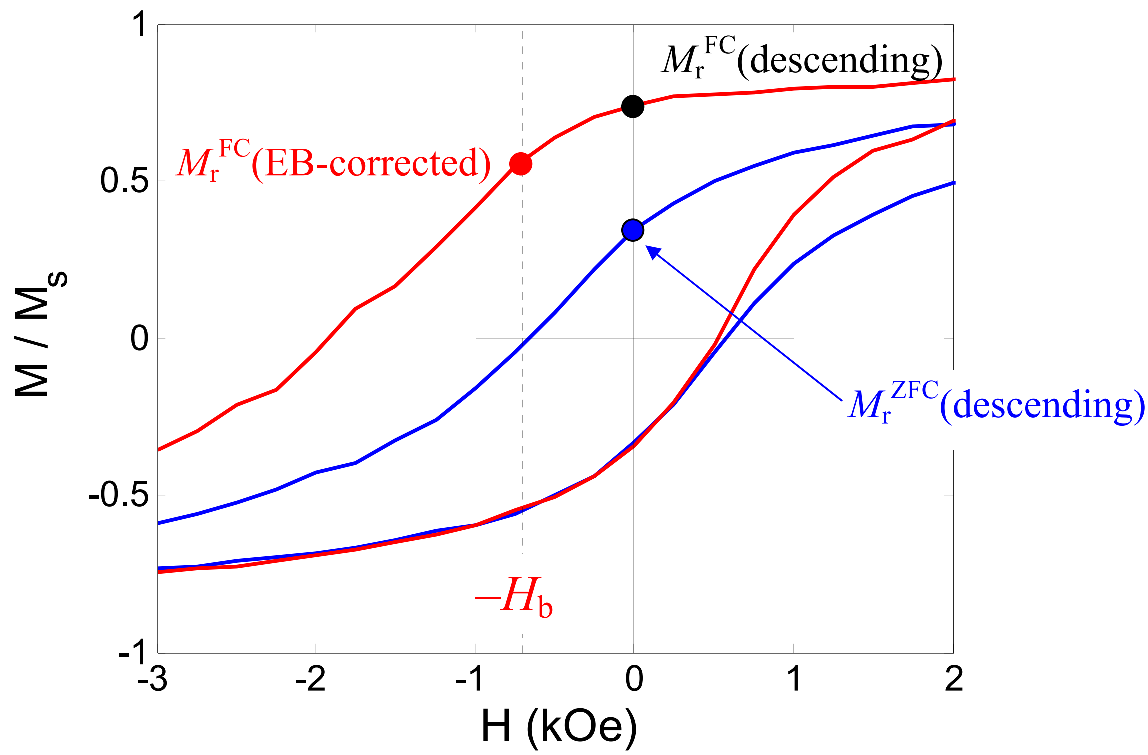

Fig. S5. The definitions of remanent magnetization M_r for FC and ZFC hysteresis loops are here shown using the descending branch of the ZFC (blue) and FC (red) magnetization isotherms of sample B_2 recorded at 5 K.

M_r (descending) is measured at $H = 0$ on the descending branch of the hysteresis loop: $M_{desc}(H{=}0)$
M_r (EB-corrected) is measured at $H = -H_b$ on the descending branch of the hysteresis loop: $M_{desc}(H{=}-H_b)$

In the ZFC loop, the definition of remanence is unambiguous:

$$M_r^{ZFC} = M_{descending}(H{=}0) = -M_{ascending}(H{=}0).$$

In the FC loop, we can distinguish the "usual" remanence $M(H{=}0)$ from the EB-corrected remanence $M_{desc}(H{=}-H_b)$ (only the remanences on the descending branch are here considered).

Comparing M_r^{FC}(descending) to M_r^{ZFC} allows one to estimate the variation of the remanence due to the overall change of the loop induced by FM/AFM exchange coupling whereas comparing

M_r^{FC}(EB-corrected) to M_r^{ZFC} allows to estimate the variation of the remanence due to the change of the loop **shape** only, cleared from the effect of the loop shift.

Definition of the shape parameters $S_{\pm}$ and $B_{\pm}$ of the switching field distribution SFD

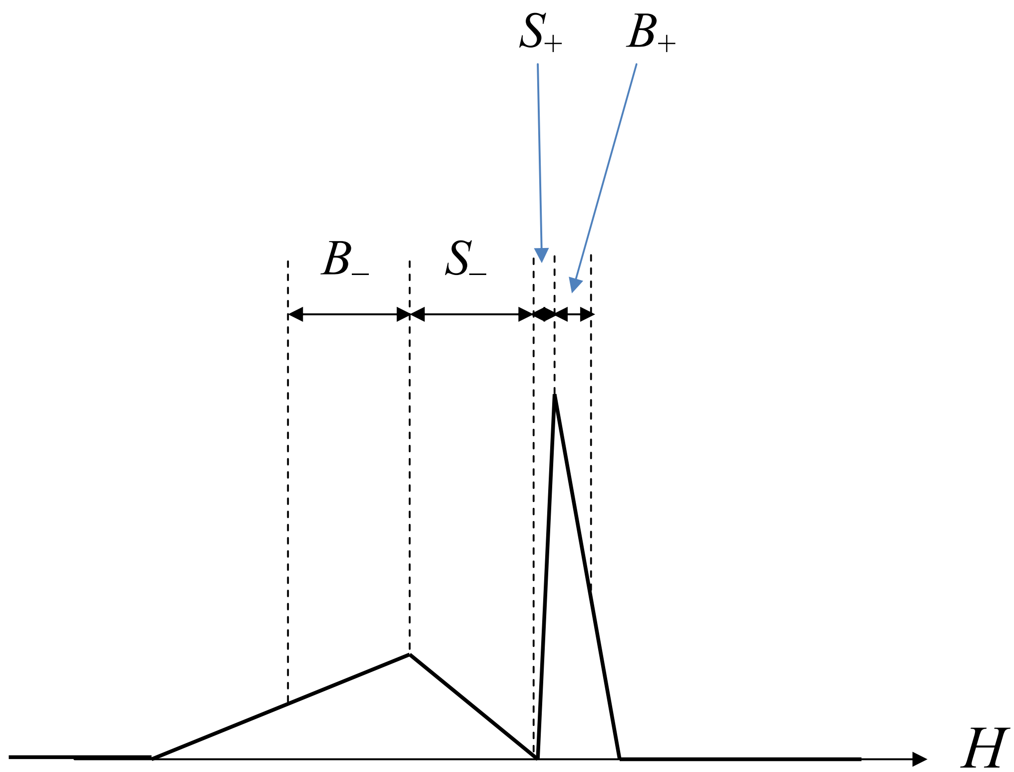

S_{+} is the field distance from the minimum of the SFD to the SFD peak in the $H > 0$ region.

S_{-} is the field distance from the minimum of the SFD to the SFD peak in the $H < 0$ region.

B_{+} is the half-width at half-height of the SFD peak in the $H > 0$ region measured towards more positive field.

B_{-} is the half-width at half-height of the SFD peak in the $H < 0$ region measured towards more negative field.

Table SII. Shape parameters $S_\pm$ and $B_\pm$ of the switching field distribution SFD calculated from ΔM.

Sample	S_- (kOe)	B_- (kOe)	S_+ (kOe)	B_+ (kOe)
A	0.5	0.6	0.5	0.5
B_1	1.2	1.2	1.0	0.7
B_2	1.5	1.2	1.0	0.6
B_3	2.0	4.0	2.3	1.5
C	1.4	1.7	1.5	0.9
D	2.5	3.7	1.6	1.0
E	2.7	3.0	1.2	0.8

S_- and B_- of samples B_3, D, and E are just estimated values because data are affected by significant uncertainty.

The dΔM/dH approximation to irreversible magnetization changes for uniaxial Stoner-Wohlfarth particles

The plots compare the true irreversible magnetization change $|(dM/dH)_{irr}|$ to $|d\Delta M/dH|$ for uniaxial Stoner-Wohlfarth particles. The latter is a good approximation to the former for all relative orientations of the applied field to the anisotropy axis.

a)

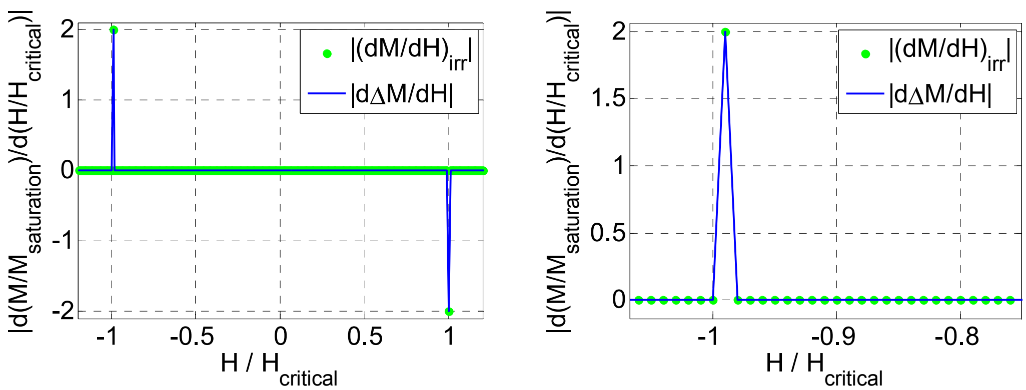

b)

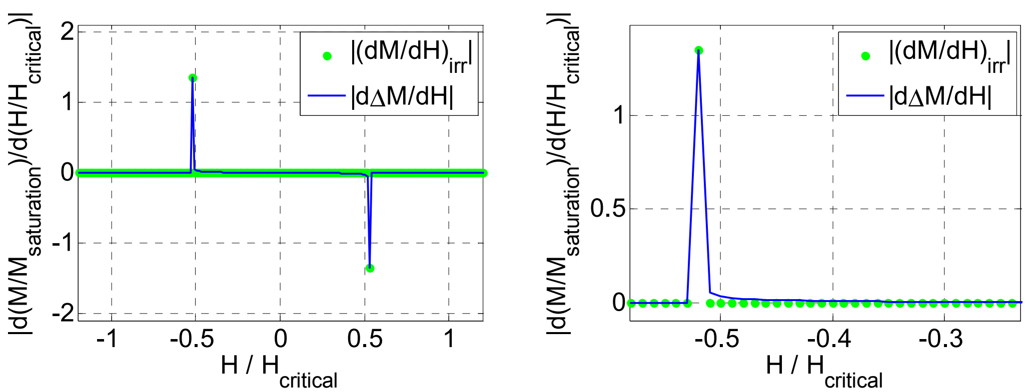

c)

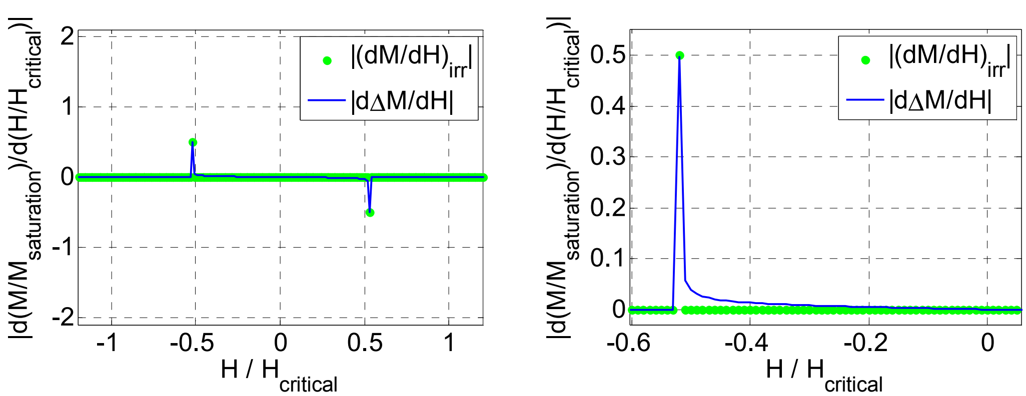

d)

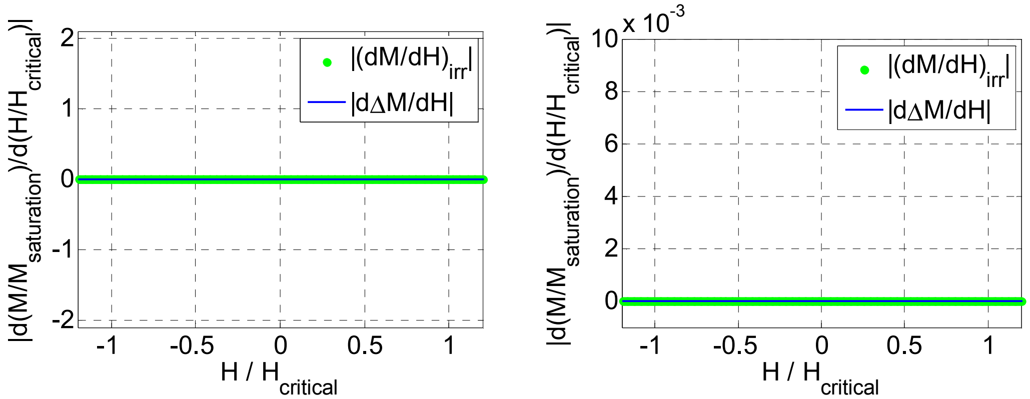

Fig. S5. Comparison of the true irreversible magnetization changes (green dots) to |dΔ*M*/d*H*| (blue line) for uniaxial Stoner-Wohlfarth particles. The angle between the applied field to the anisotropy axis is 0° (a), 30° (b), 60° (c), 90° (d). The panels on the right side portray the region close to the true switching field, when present.

Table SIII. Linear regression ($y = p\ x + q$) between the exchange bias field H_b and the coercivity H_c, remanence coercivities H_{cr}^{-} and H_{cr}^{+}, and SFD shape parameter B_{-} of thin-film assemblies of Ni@CoO core-shell NPs. The *t*- and *F*-test were carried out for the null hypothesis (*t*-test: $p = 0$ or $q = 0$, *F*-test: $R = 0$) at the 95% confidence level.

y	x	p (*t*-test) [a]	q / kOe (*t*-test) [a]	R [b]	R^2 [c]	*F*-test [a]
H_b	H_c	0.87 ± 0.06 (Y)	–0.3 ± 0.1 (Y)	0.987	0.973	Y
H_b	H_{cr}^{-}	–0.37 ± 0.01 (Y)	NA [d]	0.996	0.991	Y
H_b	H_{cr}^{+}	1.8 ± 0.2 (Y)	NA [d]	0.963	0.928	Y
H_b	B_{-}	0.61± 0.03 (Y)	NA [d]	0.995	0.989	Y

[a] Y: test passed. [b] R: linear correlation coefficient. [c] R^2: linear determination coefficient, *i.e.*, the fraction of the variation of y due to the linear association with x. [d] In this case, a proportional model $y = p\ x$ was used.

Table SIV. Regression between the exchange bias field H_b and the thickness of the oxide shell of Ni@CoO core-shell NPs. The *t*- and *F*-test were carried out for the null hypothesis (*t*-test: $p = 0$ or $q = 0$, *F*-test: $R = 0$) at the 95% confidence level.

Linear regression ($H_b = p\,x + q$) including the B_3 datum

x	p / kOe nm^{-1} (*t*-test) [a]	q / kOe (*t*-test) [a]	R [b]	R^2 [c]	*F*-test [a]
t_{NiO}	0.3 ± 1.9 (N)	1.2 ± 0.8 (N)	0.068	0.005	N
t_{CoO}	0.7 ± 0.3 (N)	0.4 ± 0.5 (N)	0.673	0.454	N
$t_{NiO} + t_{CoO}$	0.8 ± 0.3 (N)	–0.1 ± 0.6 (N)	0.754	0.569	N

Linear regression ($H_b = p\,x + q$) excluding the B_3 datum

x	p / kOe nm^{-1} (*t*-test) [a]	q / kOe (*t*-test) [a]	R [b]	R^2 [c]	*F*-test [a]
t_{NiO}	–3 ± 2 (N)	2.0 ± 0.8 (Y)	0.521	0.272	N
t_{CoO}	0.8 ± 0.2 (Y)	–0.0 ± 0.3 (N)	0.939	0.881	Y
$t_{NiO} + t_{CoO}$	0.9 ± 0.2 (N)	–0.3 ± 0.4 (N)	0.911	0.830	Y

Proportional regression ($H_b = p\,x$) excluding the B_3 datum

x	p / kOe nm^{-1} (*t*-test) [a]	R [b]	R^2 [c]	*F*-test [a]
t_{NiO}	3 ± 1 (N)	0.692	0.479	N
t_{CoO}	0.83 ± 0.07 (Y)	0.985	0.970	Y
$t_{NiO} + t_{CoO}$	0.71 ± 0.07 (Y)	0.974	0.949	Y

[a] Y: test passed; N: test not passed. [b] R: linear correlation coefficient. [c] R^2: linear determination coefficient, *i.e.*, the fraction of the variation of H_b due to the linear association with x.

Table SV. Bivariate regression of the exchange bias field H_b or the descendent remanence coercivity H_{cr}^{-} with the thickness of the oxide shells of Ni@CoO core-shell NPs. The *t*- and *F*-test were carried out for the null hypothesis (*t*-test: p_{NiO} = 0 or p_{CoO} = 0, *F*-test: R = 0) at the 95% confidence level.

Bivariate regression of EB field: $H_b = p_{NiO}\, t_{NiO} + p_{CoO}\, t_{CoO}$

	p_{NiO} / kOe nm^{-1} (*t*-test) [a]	p_{CoO} / kOe nm^{-1} (*t*-test) [a]	R [b]	R^2 [c]	*F*-test [a]
B_3 included	1.2 ± 0.8 (Y)	0.7 ± 0.2 (Y)	0.949	0.901	Y
B_3 excluded	–0.1 ± 0.5 (N)	0.9 ± 0.1 (Y)	0.985	0.970	Y

[a] Y: test passed; N: test not passed. [b] R: linear correlation coefficient. [c] R^2: linear determination coefficient, *i.e.*, the fraction of the variation of H_b due to the linear association with t_{NiO} and t_{CoO}.

Bivariate regression of descending-branch remanent coercivity: $H_{cr}^{-} = p_{NiO}\, t_{NiO} + p_{CoO}\, t_{CoO}$

	p_{NiO} / kOe nm^{-1} (*t*-test) [a]	p_{CoO} / kOe nm^{-1} (*t*-test) [a]	R [b]	R^2 [c]	*F*-test [a]
B_3 included	–3 ± 2 (Y)	–2.1 ± 0.4 (Y)	0.967	0.936	Y
B_3 excluded	0 ± 1 (N)	–2.4 ± 0.2 (Y)	0.993	0.986	Y

[a] Y: test passed; N: test not passed. [b] R: linear correlation coefficient. [c] R^2: linear determination coefficient, *i.e.*, the fraction of the variation of H_b due to the linear association with t_{NiO} and t_{CoO}.

References

[1] C. Song, B. Cui, H. Y. Yu and F. Pan, Completely inverted hysteresis loops: Inhomogeneity effects or experimental artifacts, *J. Appl. Phys.* **114**, 183906 (2013).